can be set equal to $0.55\ (p_i + p_{0.95})\ (A_{0.95} - A_i)$. (If pressure had varied linearly with area, the coefficient would have been 0.50.) Equation (1) is used to locate $A_{0.95}$. However, as the interaction region approaches the nozzle-exit plane with finite A_e, the value $(\epsilon_{0.95} - \epsilon_i)$ cannot exceed $(\epsilon_e - \epsilon_i)$ and must therefore tend to zero. This condition will be referred to as case B. In effect, as $\epsilon_i \rightarrow \epsilon_e$, the assumption that the length of the interaction region equals 10 δ is no longer valid. Some data showing this phenomenon have been plotted in Fig. 3 with the family of linear equations which has been fitted to the data

$$\epsilon_{0.95} - \epsilon_i = (\epsilon_e - \epsilon_i)/1.45 \tag{4}$$

which gives $\epsilon_{0.95} - \epsilon_i = 0$ when $\epsilon_i = \epsilon_e$, where $\epsilon_{0.95}$ corresponds to $p = 0.95\ p_a$. Solving Eqs. (1) and (4) simultaneously, we obtain the following regions of validity for cases A and B, as indicated by the upper and lower inequality signs, respectively:

$$\epsilon_i \begin{matrix} \overset{A}{\leq} \\ \underset{B}{>} \end{matrix} \frac{\epsilon_e}{1.6} + 0.38 \tag{5}$$

The region represented by

$$\int_{A_{0.95}}^{A_e} p dA$$

shows almost a constant pressure, and this term can therefore be approximated by the arithmetic average value for the region $0.975\ p_a(A_e - A_{0.95})$. Combining this with Eq. (3), we obtain the expression

$$F_{s1} = p_c A_t c_{f_i} + 0.55(p_i + p_{0.95})(A_{0.95} - A_i) - p_a(0.975 A_{0.95} + 0.025\ A_e) \tag{6}$$

The equations in this section can be used to plot nozzle performance, including flow separation, as shown in Fig. 4.

References

[1] Arens, M. and Spiegler, E., "Shock-induced boundary layer separation in overexpanded conical exhaust nozzles," AIAA J. **1**, 578–581 (1963).

[2] Chapman, D. R., Kuehn, D. M., and Larson, H. K., "Investigation of separated flows in supersonic and subsonic streams with emphasis on the effect of transition," NACA Rept. 1356, 37 (1958).

[3] Gadd, G. E., "Interactions between wholly laminar or wholly turbulent boundary layers and shock waves strong enough to cause separation," J. Aeronaut. Sci. **20**, 729–739 (1953).

[4] Bogdonoff, S. M. and Kepler, C. E., "Separation of a supersonic turbulent boundary layer," J. Aeronaut. Sci. **22**, 414–424 (1955).

[5] Liepmann, H. W., Roshko, A., and Dhawan, S., "On reflection of shock waves from boundary layers," NACA Rept. 1100 (1952).

[6] Gadd, G. E., Holder, D. W., and Regan, J. D., "An experimental investigation of the interaction between shock waves and boundary layers," Proc. Roy. Soc. (London) **A 226**, 227–253 (1954).

[7] Tucker, M., "Approximate calculation of turbulent boundary-layer development in compressible flow," NACA TN 2337 (1951).

[8] Arens, M. and Spiegler, E., "Separated flow in overexpanded nozzles at low pressure ratios," Bull. Res. Council Israel **C11**, 45 (1962).

[9] Bloomer, H. E., Antl, R. J., and Renas, P. E., "Experimental study of effects of geometric variables on performance of conical rocket exhaust nozzles," NASA TN D-846 (1961).

[10] Campbell, C. E. and Farley, J. M., "Performance of several conical convergent-divergent rocket-type exhaust nozzles," NASA TN D-467 (1960).

[11] Foster, C. R. and Cowles, F. B., "Experimental studies of gas flow separation and overexpanded exhaust nozzles for rocket motors," Jet Propulsion Lab., California Institute of Technology, Progr. Rept. 4-103 (1949).

[12] Ashwood, P. F. and Crosse, G. W., "The influence of pressure ratio and divergence angle on the shock position in two-dimensional, overexpanded, convergent-divergent nozzles," Ministry of Supply, Aeronautical Research Council, Current Paper 327 (1957).

[13] Fraser, R. P., Eisenklam, P., and Wilkie, D., "Investigation of supersonic flow separation in nozzles," J. Mech. Eng. Sci. **1**, 267 (1959).

[14] McKenney, J. D., "An investigation of flow separation in an overexpanded supersonic nozzle," Ph.D. Thesis, California Institute of Technology (1949).

[15] Ahlberg, J. H., Hamilton, S., Migdal, D., and Nilson, E. N., "Truncated perfect nozzles in optimum nozzle design," ARS J. **31**, 614 (1961).

A Kinetic Treatment of Ablation

Richard L. Newman*

Douglas Aircraft Company, Inc., Santa Monica, Calif.

Nomenclature

b = volume density of bonds
H = enthalpy
K = Boltzmann constant
m = kinetic order of the reaction
n = number of bonds in each species
$\dot{q}$ = net heat flux to the surface
t = time
T = temperature
v = recession velocity
x = distance coordinate (fixed in space)
Z = frequency factor
α = thermal diffusivity
ϵ = activation energy
Λ = number of laminae
ν = stoichiometric factor
ξ = distance coordinate (fixed with respect to the surface)
ϕ = fraction of bonds unbroken

Subscripts

A = ablation
i = ith species
n = index
R = reaction process
s = surface
0 = interior

THE present widespread use of ablation shielding for thermal protection shows a need for a basic understanding of the mechanism of ablation. Previous analytical models have either neglected chemical reactions within a decomposing material, or have had too large a scope to permit study of internal processes. This paper reports results for the quasi-steady state for relatively uncomplicated materials. Later work will extend these results, both to cover charring materials and to eliminate some of the simplifying assumptions.

Analysis

The principal mechanism of thermal degradation of a thermoplastic, noncharring polymer is the breaking of bonds in the chain. The order and extent of bond rupture will

Received July 13, 1964; revision received August 11, 1964. Prepared under the sponsorship of the Douglas Aircraft Co. Independent Research and Development Program. The author wishes to thank W. S. Rigdon for many helpful discussions, and L. E. Weems for help in preparing the manuscript.

* Research Laboratory Analyst, Astrodynamics Branch, Advance Space Technology, Missile and Space Systems Division; on leave of absence at Department of Fuel Technology, Pennsylvania State University, University Park, Pa.

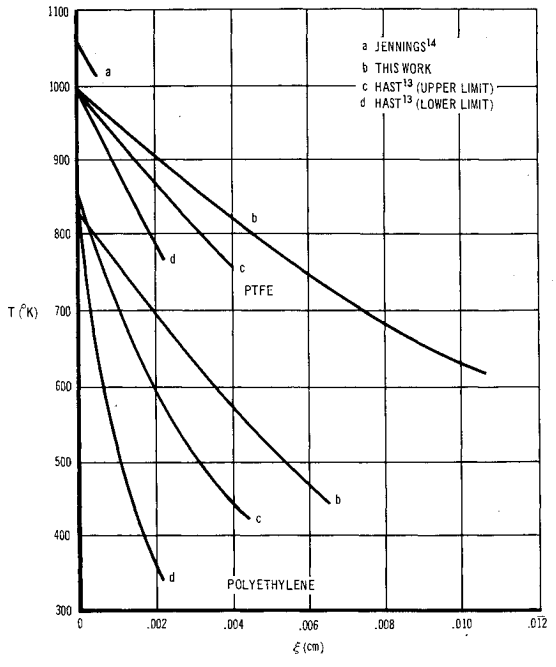

Fig. 1 Temperature profile.

vary from material to material. The bonds in the chain are presumed to obey the Arrhenius equation,

$$-d\phi/dt = \phi^m Z \exp(-\epsilon/KT) \tag{1}$$

where ϕ, the fraction of bonds not broken, refers to bonds that are in the backbone of the chain; it has an initial value of unity (no bonds broken) and will decrease as the material reacts. In general, it will not reach zero (every bond broken), because the material will cease to be a recognizable solid long before this. The ultimate value ϕ_s may be calculated from the composition of the products. For a polymer of composition $(CRH - CH_2)_n$ degrading to the monomer $CRH = CH_2$, one-half of the bonds in the backbone of the chain are broken, and $\phi_s = \frac{1}{2}$. [If this compound degrades to the dimer $(CRH - CH_2)_2$, ϕ_s will be $\frac{3}{4}$.] In general, if n_i is the number of bonds derived from the backbone of the polymer chain in the ith product, and ν_i is the mole fraction of that species, then

$$\phi_s = \sum_i \nu_i n_i/(n_i + 1) \tag{2}$$

The course of the reaction may be followed by reference to ϕ.

The model considered here is a semi-infinite slab with a heat flux applied to the surface. The material is assumed to have reached a quasi-steady-state condition, which implies a constant degradation rate, a steady recession of the surface, and a fixed thermal profile with respect to the surface. No phase changes are assumed to occur within the material.

The physical picture of the process may be thought of as a reacting material (the polymer) moving through a thermal profile and, at the surface, being completely degraded into a gas. The total enthalpy change associated with this reaction, ΔH_R, is found by

$$\Delta H_R = [H_{\text{products}}]_{Ts} - [H_{\text{polymer}}]_{T_0} \tag{3}$$

From this, the recession rate of the surface may be obtained easily:

$$v = \dot{q}/b\ \Delta H_R \tag{4}$$

It is convenient to transform to a coordinate that is fixed with respect to the surface,

$$\xi = x - vt \tag{5}$$

Now, from Eqs. (1) and (5)

$$d\phi/d\xi = \phi^m Z \exp(-\epsilon/KT)/v \tag{6}$$

The exponent m may be taken as unity for most polymeric degradation reactions.

In treating the reaction, constant temperature will be approximated by taking small laminae. In each lamina, the amount of reaction occurring may be found by integrating Eq. (6) at constant temperature:

$$\ln[(\phi - \delta\phi)/\phi] = -[Z \exp(-\epsilon/KT)v]\delta\xi \tag{7}$$

ϕ now is a function of two variables, T and ξ. Harmon and Myers[1] indicate that the temperature profile for a reacting solid is exponential

$$T(\xi) = T_s \exp(-v\xi/\alpha) \tag{8}$$

if all of the heat is absorbed at the surface, which is a fair approximation.

With temperature as the independent variable, it is possible to solve for ϕ as a function of temperature only. Also, dividing the material into laminae based on equal temperature intervals will provide narrow laminae near the surface, where the slope is the steepest, and where most of the reaction occurs. Equation (7) with temperature as the independent variable becomes

$$\ln[(\phi - \delta\phi)/\phi] = [\alpha Z \exp(-\epsilon/KT)/v^2T]\delta T \tag{9}$$

$$\delta\phi = \phi\{1 - \exp[\alpha Z \exp(-\epsilon/KT)/v^2T\delta T]\} \tag{9a}$$

The boundary conditions that must be satisfied are, at the surface, $\phi = \phi_s$ and $T = T_s$; and in the interior, $\phi \to 1$, as $T \to T_0$.

Since the surface temperature is not known a priori and is required to evaluate ΔH_R, a trial value is assumed. The correct value for the surface temperature will be indicated by satisfaction of the remaining boundary conditions.

This analysis has been programed on an IBM 7094 computer. An initial value of the surface temperature is assumed, and laminae are determined by

$$\delta T = (T_s - T_0)/\Lambda \tag{10}$$

where Λ is the desired number of laminae. T_n is found by

$$T_n = T_{n-1} - \delta T \tag{10a}$$

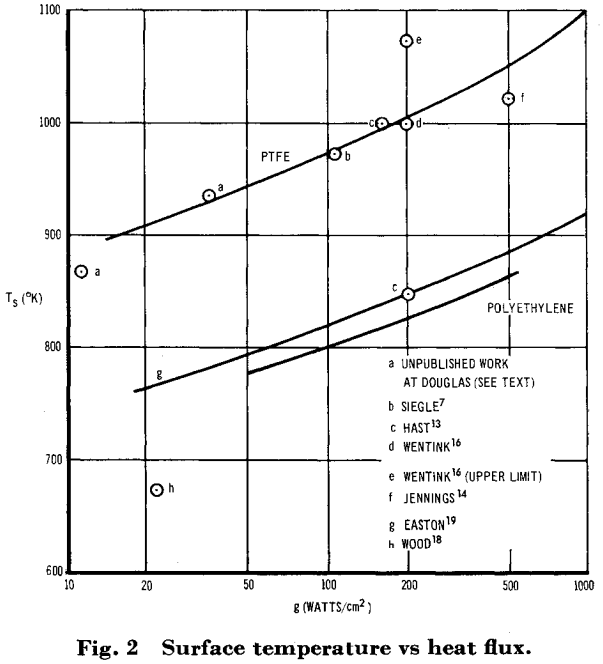

Fig. 2 Surface temperature vs heat flux.

Table 1 Heats of ablation

Material	H_A, cal/g at $\dot{q}$ = 50 w/cm²	H_A, cal/g 500 w/cm²
Polytetrafluoroethylene (PTFE)	282.4	283.7
Polyethylene	24.5	28.6
Polypropylene	401	...

and ϕ_n and ξ_n are found from Eqs. (9a) and (8). If ϕ_0 is sufficiently close to unity, the solution is presumed correct. If not, a new value of T_s is estimated. The first three values of T_s are chosen by incrementing T_s. Subsequent values of T_s are estimated from the last three values of T_s, the last three values of ϕ_0, and the desired value of unity (for ϕ_0) with a parabolic-curve-fit expression.

Results and Conclusions

For polytetrafluoroethylene (PTFE), the values for the physical constants were obtained from Sperati and Starkweather[2] and the heat capacity from Mark and Dole.[3] The kinetics of degradation have been studied by several authors.[4–8] Since these results were in fairly close agreement, values of 78,000 and 5×10^{18} were chosen for ϵ and Z. The products were chosen to be 97% monomer, 2.9% sesquimer (C_3F_6), and 0.1% dimer. The heats of formation were obtained from Duus,[9] and the heat capacity of the fragments calculated using the method given in Ref. 10. For polyethylene, the handbook values[11] were used for physical constants and kinetics were obtained from Madorsky.[12] The heat of reaction and heat capacity were estimated.[10] Two parameters may be used to compare calculated results with the actual behavior: the temperature profile (usually, just the surface temperature), and the heat of ablation. Of these, the surface temperature is the most useful, because it may be measured directly.

Measured thermal profiles[13] of polytetrafluoroethylene and polyethylene are compared with those calculated in Fig. 1, and surface temperatures as functions of heat flux are shown in Fig. 2. To supplement the literature values for surface temperature, some measurements have been made for polytetrafluoroethylene (commercial Teflon) in an arc-image furnace. These are shown in Fig. 2. The heat flux was estimated using the calculated radiant energy and Wentink's value for absorption coefficient.[15]

The heat of ablation may be defined in many ways. A typical definition might be the difference in heat absorbed by a bare metal body with and without protection. Such a definition includes many effects not directly related to the degradation reaction within the material. The heat of ablation ΔH_A is defined herein as the total enthalpy change of the material, i.e., $\Delta H_A = \Delta H_R$.

This value (Table 1) will, in general, be lower than measured values and should only be considered as an indication of the relative merits of two materials. The calculated results show good agreement with the available experimental data. However, there is some variation in the literature data to be input to the program. For this reason, results were calculated for all available values for the required input data for PTFE. All quantities, except the heat of reaction and the kinetic constants, showed negligible effects (<10° in T_s). Table 2 shows the effect of small changes in ϵ, Z, and H_0.

Table 2 Effect of input data on surface temperature[a]

Z (sec^{-1})	ΔH_0 (cal/mole)	ϵ (cal/mole)	T_s(°K)
5×10^{19}[b]	58,625[b]	78,000[b]	998.5
5×10^{19}	40,000	78,000	1019.2
5×10^{19}	75,000	78,000	961.2
5×10^{19}	58,625	85,000	1089.8
10^{18}	58,625	78,000	1041.9

[a] Polytetrafluoroethylene (PTFE) $\dot{q}$ = 200 w/cm².
[b] Standard values.

Programing parameters, such as number of laminae and precision in comparing ϕ_0 to unity were adjusted to the point of diminishing returns. Values of $\Lambda = 25$ and $\phi_0 = 1 \pm 0.0001$ were used, and the resultant surface temperatures were only slightly higher for $\Lambda = 250$. Larger errors in comparing ϕ_0 to unity will decrease the precision of the calculated surface temperature.

The assumption of quasi-steady-state conditions has obvious attractiveness due to the ease of calculation. Since the time during which the material undergoes degradation is quite small (<0.1 sec for PTFE at typical heat fluxes), a qualitative argument may be advanced for this assumption. This time is very short compared with the duration of ablation. A similar argument is offered for the semi-infinite slab assumption. The distance from the surface at which the material is still at T_0 is very short compared with the thickness of most samples.

The comparison of measured and calculated thermal profiles shows that the exponential profile yields values that are somewhat higher than those measured by Hanst.[13] Additional calculations are under way at present to eliminate the assumption of an exponential profile.

Extension of this model to charring materials is envisioned as being divided into two parts. The first, dealing with the prechar region, will be essentially similar to this analysis. That part may, for example, treat different kinds of bonds separately, with both degrading and cross-linking reactions. In the second, the char region will deal with percolation of hot gases through the char, including reactions with the environment.

References

[1] Harmon, D. B. and Myers, H., "Energy transfer processes in decomposing polymeric systems," Douglas Aircraft Co., Engineering Paper 1020 (1960).

[2] Sperati, C. A. and Starkweather, H. A., "Fluorine containing polymers," Fortschr. Hochpolymer. Forsch. II, 465–495 (1961).

[3] Mark, P. and Dole, M., "Specific heat of polytetrafluoroethylene," J. Am. Chem. Soc. **77**, 4771 (1955).

[4] Madorsky, S., L. Hart, V. E., Straus, S., and Sedlak, V. A., "Pyrolysis of polytetrafluoroethylene and hydrofluoroethylene polymers in vacuum," J. Res. Nat. Bur. Std. **51**, 327–333 (1953).

[5] Lewis, E. and Naylor, M., "Pyrolysis of polytetrafluoroethylene," J. Am. Chem. Soc. **69**, 1968–1970 (1947).

[6] Anderson, H. C., "Pyrolysis of polytetrafluoroethylene," Makromol. Chem. **51**, 233–235 (1962).

[7] Siegle, J. C. and Muus, L. T., "Pyrolysis of polytetrafluoroethylene," 150th National Meeting of the American Chemical Society (1956).

[8] Straus, S. and Madorsky, S., "Pyrolysis of some polyvinyl polymers at temperatures to 1200 deg. C," J. Res. Nat. Bur. Std. **66A**, 401–406 (1962).

[9] Duus, H. C., "Thermochemical studies on fluorocarbons," Ind. Eng. Chem. **47**, 1445–1449 (1955).

[10] Janz, G. J., *Estimation of Thermodynamic Properties of Organic Compounds* (Academic Press Inc., New York, 1958), pp. 58 ff.

[11] "Materials Selector Issue," Mater. Design Eng. **58**, 218 (1963).

[12] Madorsky, S. L., "Rates of thermal degradation of polystyrene and polyethylene in a vacuum," J. Polymer Sci. **9**, 133–156 (1952).

[13] Hanst, P. L., "Surface temperature measurements on ablating missile and satellite heat shield materials," *Temperature—Its Measurements and Control in Science and Industry* (Reinhold Publishing Corp., New York, 1962) pp. 489–496.

[14] Jennings, R. L. and Easton, C. R., "The surface temperature of ablating teflon," Douglas Rept. SM 35759 (May 1959).

[15] Wentink, T. and Planet, W. G., "The infrared transmittance and emittance of polytetrafluoroethylene," J. Opt. Soc. Am. **51**, 601–602 (1961).

[16] Wentink, T., private communication, Avco Co., Wilmington, Mass. (August and December 1963).
[17] Settlage, P. H. and Siegle, J. C., "Behavior of 'Teflon' fluorocarbon resins at elevated temperatures," *Physical Chemistry in Aerodynamic and Space Flight* (Pergamon Press, London, 1961), pp. 73–81.
[18] Wood, R. M. and Tagliani, R. J., "Heat protection by ablation," Aero/Space Eng. **19**, 32 (1960).
[19] Easton, C. R., private communication, Douglas Aircraft Co.

Some Aspects of the Applications of Hybrid Propulsion Systems

A. L. Wahlquist* and G. C. Panelli†
Lockheed Propulsion Company, Redlands, Calif.

HYBRID propulsion systems using solid fuels and liquid oxidizers possess possibilities for high performance with simplicity and resulting reliability. Unclassified chemical data indicate that some hybrid propellants will provide theoretical vacuum specific impulse values of about 500 lb-sec/lb. When reasonable combustion and nozzle efficiencies are applied to this theoretical value, the potential delivered performance is still very high. Most effort to date has been in the areas of experimental and theoretical work on the burning mechanism and the performance for various propellant combinations. Consideration must also be given to the application of hybrids to the specific requirements of a vehicle system. Several aspects of hybrid propulsion system applications come to light when quantitative mission requirements and related vehicles are analyzed. Two of the more interesting aspects, namely, the requirement for achieving constant thrust and wide throttling, are the subjects of this note.

Regression Rate

Hybrid combustion is dependent on the liquid oxidizer flow and the solid fuel burning or regression rate. The regression-rate expression that relates the pertinent ballistic parameters is of the general form:

$$r = BG_T^x/L_p^y + C$$

where r is the regression rate, L_p is the grain port length B is the convection heat-transfer constant, y is the grain port length exponent, x is the mass flux exponent, C is the constant, and G_T is the total mass flow rate per square inch of grain port area (mass flux).

This expression can be derived explicitly for different propellant combinations and fuel grain configurations to fit available experimental and theoretical data. Its empirically determined constants are influenced by the propellant combination and the temperature at combustion conditions. To illustrate how the various parameters affect the O/F ratio (oxidizer-to-fuel weight ratio), regression rate, and total weight flow, the general regression-rate expression was made explicit for a circular port grain. Assuming a constant oxidizer flow rate, specific values for x and y, and ignoring the constant C, the O/F varies with the relationship $K_1 = (O/F)(O/F + 1)^4 L_p^4/D_p^3$; the regression rate varies with the relationship $r = K_2(O/F + 1)^4 L_p^3/D_p^4$; and the total flow rate (and therefore thrust) varies with the expression $\dot{W}_T = K_3(O/F + 1)^5 L_p^4/D_p^3$, where D_p is the fuel grain port diameter.

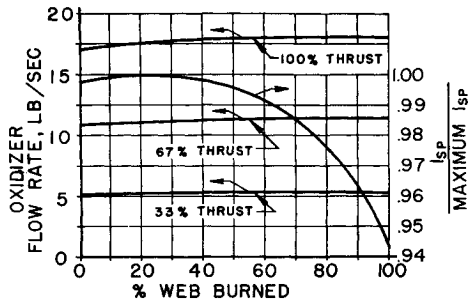

Fig. 1 Oxidizer flow rate and specific impulse.

Constant Thrust

The preceding expressions indicate that, as the port diameter increases during burning, the only way to maintain constant thrust is to vary the O/F ratio. Control of the O/F ratio is accomplished by varying the oxidizer flow rate. Figure 1 shows the variation in oxidizer flow rate required to achieve constant thrust for a hypothetical design and the resultant variation in specific impulse. The theoretical change in I_{sp} with O/F and P_c can be seen from Fig. 2, which is typical of the ballistic performance of all rocket systems. This requirement to vary the oxidizer flow rate somewhat complicates an otherwise extremely simple system. We therefore will examine the consequences of operating the motor with a constant oxidizer flow rate, which reflects the minimum complexity system when an absolutely constant thrust level is not required. The burning time is under 200 sec, and no throttling is specified. Restart capability is not discussed in this note, although it is easily accomplished by the use of a hypergolic hybrid propellant combination.

Several possible grain designs can be considered for the hybrid engine. Since the star design permits a smaller length-to-diameter ratio than does the circular port and is generally simpler than the other types, it was selected for the analysis of the effect of constant oxidizer flow rate on thrust and I_{sp}. The simple internal ballistic equations are only slightly more complex with respect to the geometrical parameters. A constant perimeter, eight-point star configuration with constant oxidizer flow rate produces a thrust that varies less than 12% (Fig. 3). The average I_{sp} for the total burning time varies less than 0.3% from the nominal value at optimum O/F. Although the O/F ratio varies, complete (within reasonable expulsion and sliver tolerances) propellant utilization poses no problem because the proper amounts of both fuel and oxidizer can be predetermined and the propulsion system loaded accordingly.

Wide Throttling

A hybrid engine capable of 50/1 throttling represents the other end of design complexity. With oxidizer injected at the head end only, 50/1 throttling would require varying

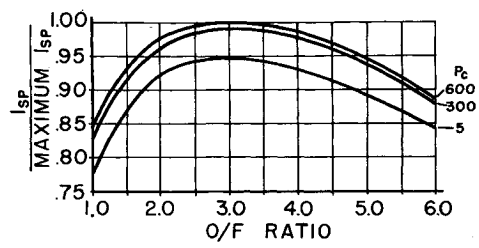

Fig. 2 Theoretical kinetic specific impulse.

Presented as Preprint 64-225 at the 1st AIAA Annual Meeting, Washington, D. C., June 29–July 2, 1964; revision received December 11, 1964.
* Senior Engineer.
† Manager, Advanced Design and Analysis. Member AIAA.